



# WWP1 knockout in mice exacerbates obesity-related phenotypes in white adipose tissue but improves whole-body glucose metabolism

Shunsuke Hoshino<sup>1</sup>, Masaki Kobayashi<sup>1</sup> , Ryoma Tagawa<sup>1</sup>, Ryutaro Konno<sup>1</sup>, Takuro Abe<sup>1</sup>, Kazuhiro Furuya<sup>1</sup>, Kumi Miura<sup>1</sup>, Hiroki Wakasawa<sup>1</sup>, Naoyuki Okita<sup>2</sup>, Yuka Sudo<sup>1</sup>, Yuhei Mizunoe<sup>3</sup>, Yoshimi Nakagawa<sup>3</sup>, Takeshi Nakamura<sup>4</sup> , Hiroshi Kawabe<sup>5,6,7</sup> and Yoshikazu Higami<sup>1</sup>

<sup>1</sup> Laboratory of Molecular Pathology and Metabolic Disease, Faculty of Pharmaceutical Sciences, Tokyo University of Science, Noda, Japan

<sup>2</sup> Division of Pathological Biochemistry, Faculty of Pharmaceutical Sciences, Sanyo-Onoda City University, Sanyo-onoda, Japan

<sup>3</sup> Department of Internal Medicine (Endocrinology and Metabolism), Faculty of Medicine, University of Tsukuba, Tsukuba, Japan

<sup>4</sup> Division of Biosignaling, Research Institute for Biomedical Sciences, Tokyo University of Science, Noda, Japan

<sup>5</sup> Department of Molecular Neurobiology, Max Planck Institute of Experimental Medicine, Göttingen, Germany

<sup>6</sup> Division of Pathogenic Signaling, Department of Biochemistry and Molecular Biology, Kobe University Graduate School of Medicine, Chuo-ku, Kobe, Japan

<sup>7</sup> Department of Gerontology, Laboratory of Molecular Life Science, Institute of Biomedical Research and Innovation, Foundation for Biomedical Research and Innovation at Kobe, Japan

## Keywords

white adipose tissue; obesity; WWP1; antioxidative capacity; mitochondrial function

## Correspondence

M. Kobayashi and Y. Higami, Laboratory of Molecular Pathology & Metabolic Disease, Faculty of Pharmaceutical Sciences, Tokyo University of Science, 2641 Yamazaki, Noda, Chiba, 278-8510, Japan  
Tel/Fax: +81 4 7121 3676  
E-mail: kobayashim@rs.tus.ac.jp (MK) and higami@rs.noda.tus.ac.jp (YH)

Shunsuke Hoshino and Masaki Kobayashi contributed equally to this work

(Received 11 November 2019, revised 27 December 2019, accepted 16 January 2020)

doi:10.1002/2211-5463.12795

White adipose tissue (WAT) is important for maintenance of homeostasis, because it stores energy and secretes adipokines. The WAT of obese people demonstrates mitochondrial dysfunction, accompanied by oxidative stress, which leads to insulin resistance. WW domain-containing E3 ubiquitin protein ligase 1 (WWP1) is a member of the HECT-type E3 family of ubiquitin ligases and is associated with several diseases. Recently, we demonstrated that WWP1 is induced specifically in the WAT of obese mice, where it protects against oxidative stress. Here, we investigated the function of WWP1 in WAT of obese mice by analyzing the phenotype of *Wwp1* knockout (KO) mice fed a high-fat diet. The levels of oxidative stress markers were higher in obese WAT from *Wwp1* KO mice. Moreover, *Wwp1* KO mice had lower activity of citrate synthase, a mitochondrial enzyme. We also measured AKT phosphorylation in obese WAT and found lower levels in *Wwp1* KO mice. However, plasma insulin level was low and glucose level was unchanged in obese *Wwp1* KO mice. Moreover, both glucose tolerance test and insulin tolerance test were improved in obese *Wwp1* KO mice. These findings indicate that WWP1 participates in the antioxidative response and mitochondrial function in WAT, but knock-down of WWP1 improves whole-body glucose metabolism.

## Abbreviations

4-HNE, 4-hydroxy-2-nonenal; CBB, Coomassie Brilliant Blue; CoxII, cytochrome c oxidase subunit II; CS, citrate synthase; DTNB, 5,5-dithio-bis-(2-nitrobenzoic acid); GTT, glucose tolerance test; HFD, high-fat diet; Hprt, hypoxanthine guanine phosphoribosyl transferase; ITT, insulin tolerance test; KLF2, Kruppel-like factor 2; KLF5, Kruppel-like factor 5; KO, knockout; mtDNA, mitochondrial DNA; ND, normal diet; OCR, oxygen consumption rate; Ppar $\gamma$ , peroxisome proliferator-activated receptor  $\gamma$ ; PTEN, phosphatase and tensin homolog; ROS, reactive oxygen species; Rps18, ribosomal protein S18; Sod1, superoxide dismutase 1; Sod2, superoxide dismutase 2; SPG20, spastic paraplegia 20; TCA cycle, tricarboxylic acid cycle; TGF $\beta$ , transforming growth factor  $\beta$ ; TNB, thio-bis-(2-nitrobenzoic acid); Trx1, thioredoxin 1; Trx2, thioredoxin 2; WAT, white adipose tissue; WT, wild-type; WWP1, WW domain-containing E3 ubiquitin protein ligase 1.

White adipose tissue (WAT) is important for maintenance of homeostasis, because it stores energy in the form of triglyceride and secretes adipokines that affect energy metabolism by modulating the activities of adiponectin, leptin, and proinflammatory cytokines. The main component of WAT is white adipocytes containing unilocular lipid droplets that hypertrophy and store excess lipid under conditions of obesity. Hypertrophy of mature adipocytes disrupts the balance in adipokine secretion, as it is accompanied by reduction in adiponectin secretion and increased release of proinflammatory cytokines that induce systemic insulin resistance, chronic inflammation, and oxidative stress [1,2].

Reactive oxygen species (ROS) are generated primarily in mitochondria and affect numerous signaling pathways [3–5]. Generally, oxidative stress is caused when the quantity of ROS generated exceeds the capacity of the antioxidant defense systems, which can result in inflammation and cell death [6,7]. Higher concentrations of ROS in WAT are closely associated with obesity-related pathologies such as hypertension, type 2 diabetes, and dyslipidemia [8,9]. Mitochondrial enzymes, which include those of the tricarboxylic acid cycle (TCA cycle), the  $\beta$ -oxidation process, and the electron transfer system, are important for both aerobic ATP synthesis and production of ROS. Mitochondrial dysfunction disrupts aerobic metabolism, which increases ROS production and impairs energy homeostasis. Mitochondria in WAT of obese people produce more ROS and express increased levels of markers of oxidative damage [10]. These observations indicate that oxidative stress because of increased mitochondrial ROS contributes to obesity-related pathologies.

WW domain-containing E3 ubiquitin protein ligase 1 (WWP1), also known as TIUL1 or AIP5, belongs to the HECT-type E3 ubiquitin ligase family. WWP1 has a C2 domain at its N-terminal and four WW domains in its central region [11,12]. The C2 domain determines subcellular localization of the molecule, while the WW domains bind to proline-rich sequences (PY motif) of substrate proteins. WWP1 has been reported to be associated with various diseases. For example, WWP1 is highly expressed in high-grade breast cancer with poor prognosis [13], whereas low expression of WWP1 protein is associated with sarcopenia and abnormal neurogenesis [14–16]. Therefore, it is likely that the pathophysiologic roles of WWP1 differ between normal and cancerous tissues.

The substrates of WWP1 include Kruppel-like factor 2 (KLF2) [17], KLF5 [18,19], and spastic paraplegia 20 (SPG20) [20,21]. It is known that KLF2 and KLF5 are involved in adipocyte differentiation [18,22], while SPG20 regulates the size and number of lipid droplets

[20]. Therefore, it is likely that WWP1 is involved in determining the phenotype of adipocytes.

Recently, we found that WWP1 is induced specifically in obese mouse WAT and is protective against oxidative stress in adipocytes [23]. However, we did not provide *in vivo* evidence for the roles of WWP1 in WAT. Therefore, in the present study, we explored the function of WWP1 in obese WAT and whole-body glucose metabolism by analyzing the phenotype of obese *Wwp1* knockout (KO) mice.

## Materials and methods

### Animals

Animal experiments were approved by the Ethics Review Committee for Animal Experimentation at Tokyo University of Science (approval number: Y19054). Mice with global KO of *Wwp1* (*Wwp1*<sup>-/-</sup> mice) and wild-type (WT) *Wwp1*<sup>+/+</sup> mice were generated by mating *Wwp1*<sup>fl/fl</sup>/*Wwp2*<sup>+/+</sup> (*Wwp1*<sup>fl/fl</sup>) mice, which were obtained by crossing *Wwp1*<sup>fl/+</sup>/*Wwp2*<sup>fl/+</sup> mice with CAG-Cre mice. *Wwp1*<sup>fl/fl</sup>/*Wwp2*<sup>fl/fl</sup> mice were provided by Dr. Hiroshi Kawabe (Max Planck Institute of Experimental Medicine, Göttingen, Germany) [16], and CAG-Cre mice were kindly provided by Dr. Takeshi Nakamura (Research Institute for Biomedical Sciences, Tokyo University of Science, Chiba, Japan). *Wwp1*<sup>fl/+</sup>/*Wwp2*<sup>fl/+</sup> mice were obtained by crossing *Wwp1*<sup>fl/fl</sup>/*Wwp2*<sup>fl/fl</sup> and C57/BL6 mice. Genotyping of offspring was performed by PCR using KOD FX neo (Toyobo, Osaka, Japan) or Quick Taq<sup>®</sup> HS DyeMix (Toyobo). Primers used for genotyping were as follows: *Wwp1*<sup>fl/fl</sup> (forward, 5'-AGA GGC AAG AGA ATG GCG TCA AG-3'; reverse, 5'-CAG AAA CAG TGA TCT ACA AGT CTA AAT G-3'), *Wwp2*<sup>fl/fl</sup> (forward, 5'-GAT GGT TGT GAG CCA CTT ACT TC-3'; reverse, 5'-CCA TCA TGA ACT TCA GCC TC-3'), *Wwp1*<sup>-/+</sup> (forward, 5'-AGA GGC AAG AGA ATG GCG TCA AG-3'; reverse, 5'-GGA GGT GAA AGG GTT GGA AGA ATA C-3'), and CAG-Cre (forward, 5'-ACC TGA AGA TGT TCG CGA TTA TCT-3'; reverse, 5'-ACC GTC AGT ACG TGA GAT ATC TT-3').

Mice were maintained under specific-pathogen-free conditions at 23°C, under a 12-h light/dark cycle in the animal facility at the Faculty of Pharmaceutical Sciences, Tokyo University of Science. They had free access to water and were fed a Charles River Formula-1 diet (21.9% crude protein, 5.4% crude fat, and 2.9% crude fiber; Oriental Yeast, Japan). At 5 weeks old, WT and KO mice were allocated to two groups: the normal diet (ND) group or high-fat diet (HFD) group. Labo MR Stock and High-Fat Diet 32 (25.5% crude protein, 32.0% crude lipid, and 2.9% crude fiber; CREA, Tokyo, Japan) were fed as the ND and HFD, respectively. At 13 weeks old, mice were euthanized under isoflurane anesthesia (Mylan, Canonsburg, PA, USA) in a fed state, and their epididymal WAT depots and

liver were collected and weighed. These tissues were immediately diced, frozen in liquid nitrogen, and stored at  $-80^{\circ}\text{C}$ . Blood samples were mixed with 100 mM EDTA in 1.5-mL microtubes and centrifuged at  $2,500 \times g$  for 10 min at  $4^{\circ}\text{C}$ , and plasma was collected and stored at  $-80^{\circ}\text{C}$  until analysis.

### Cell lines

3T3-L1 preadipocytes were purchased from RIKEN Bioresource Center (Ibaraki, Japan). 3T3-L1/shGFP and 3T3-L1/shWwp1 preadipocytes were previously established in our laboratory using a retrovirus system [23].

### Cell culture and differentiation

3T3-L1 preadipocytes were maintained in Dulbecco's modified Eagle's medium (low glucose) (Wako, Osaka, Japan) containing 10% fetal bovine serum (Thermo; Waltham, MA, USA) and 1% penicillin/streptomycin (Millipore Sigma, St. Louis, MO, USA). Differentiation of 3T3-L1 preadipocytes to adipocytes was performed as previously described [24].

### Immunoblotting

The preparation of WAT lysates and immunoblotting was performed according to our previously reported methods [24]. Briefly, WAT was lysed in SDS sample buffer (50 mM Tris-HCl (pH 6.8), 2% SDS, 3 M urea, 6% glycerol), boiled for 5 min, and sonicated. Lysates were subjected to SDS/PAGE (15  $\mu\text{g}$  protein per well), and separated proteins were transferred to nitrocellulose membranes. Membranes were blocked with blocking solution (2.5% skim milk, 0.25% BSA in TTBS) (25 mM Tris-HCl pH 7.4, 140 mM NaCl, 2.5 mM KCl, 0.1% Tween-20) for 1 h at room temperature and then probed with appropriate primary antibodies overnight at  $4^{\circ}\text{C}$ . The anti-WWP1 antibody was originally generated in our laboratory [23], anti-phospho-Akt (Ser473; #9271) and anti-Akt antibodies (#9272) were from Cell Signaling Technology (Danvers, MA, USA), and the anti-4-hydroxy-2-nonenal (4-HNE) antibody was from JaICA (MHN-020P; Shizuoka, Japan). Since the anti-4-HNE antibody nonspecifically recognizes 4-HNE-modified proteins, 4-HNE intensity was analyzed over the entire area per well on an immunoblotting membrane. Subsequently, membranes were incubated with appropriate secondary antibodies for 1 h at room temperature [horseradish peroxidase-conjugated F(ab')<sub>2</sub> fragment of goat anti-mouse IgG or anti-rabbit IgG (Jackson Immuno Research, West Grove, PA, USA)]. Antibody-bound proteins were visualized using ImmunoStar LD Reagent (Wako) and an LAS3000 Image Analyzer (Fuji-film, Tokyo, Japan), and data were analyzed using MULTIGAUGE software (GE Healthcare, Madison, WI, USA).

The intensity of Coomassie Brilliant Blue (CBB) staining of membrane proteins was used to normalize target protein expression levels.

### Quantitative real-time RT-PCR

Total RNA was extracted from frozen WAT using ISOGEN II (Nippon gene, Toyama, Japan), and reverse transcription was performed using ReverTra Ace<sup>®</sup> qPCR RT Master Mix (Toyobo). Quantitative real-time PCR was performed using the CFX Connect<sup>™</sup> Real Time System (Bio-Rad, Hercules, CA, USA) and Thunderbird SYBR qPCR mix (Toyobo), according to manufacturer protocols. Sequences of primers used for PCR are as follows: *Adiponectin* (*Adipoq*) (forward, 5'-TGC CGA AGA TGA CGT TAC TAC AAC-3'; reverse, 5'-CTT CAG CTC CTG TCA TTC CAA C-3'), *Catalase* (forward, 5'-CCA AGG CAA AGG TGT TTG AG-3'; reverse, 5'-GGG TTT CTC TTC TGG CTA TGG-3'), *Leptin* (forward, 5'-CCA GGA TCA ATG ACA TTT CAC ACA C-3'; reverse, 5'-CAG GGA GCA GCT CTT GGA GAA G-3'), *Peroxiredoxin1* (*Prdx1*) (forward, 5'-GCT TTC AGT GAT AGA GCC GAT G-3'; reverse, 5'-CCA TAA TCC TGA GCA ATG GTG-3'), *Peroxisome Proliferator-Activated Receptor  $\gamma$*  (*Ppar $\gamma$* ) (forward, 5'-CAC AAT GCC ATC AGG TTT GG-3'; reverse, 5'-GCG GGA AGG ACT TTA TGT ATG AG-3'), *Ribosomal Protein S18* (*Rps18*) (forward, 5'-TGC GAG TAC TCA ACA CCA ACA T-3'; reverse, 5'-CTT TCC TCA ACA CCA CAT GAG C-3'), *Superoxide dismutase 1* (*Sod1*) (forward, 5'-GGA TGA AGA GAG GCA TGT TGG-3'; reverse, 5'-TTT GCC CAA GTC ATC TTG TTT C-3'), *Superoxide dismutase 2* (*Sod2*) (forward, 5'-CCC AAA GGA GAG TTG CTG GAG-3'; reverse, 5'-CGA CCT TGC TCC TTA TTG AAG C-3'), *Thioredoxin1* (*Trx1*) (forward, 5'-AGC TGA TCG AGA GCA AGG AAG-3'; reverse, 5'-ATT TTG CAA GGT CCA CAC CAC-3'), and *Thioredoxin2* (*Trx2*) (forward, 5'-TTC ATG CAC AGT GGT GTG G-3'; reverse, 5'-TCA ATG GCA AGG TCT GTG TG-3'). *Rps18* was used as a housekeeping gene.

### Plasma biochemical analyses

Plasma glucose, insulin, and leptin levels were measured using Autokit Glucose (Wako), a Mouse Insulin ELISA KIT (Utype) (Shibayagi, Japan), and a Quantikine<sup>®</sup> ELISA Mouse/Rat Leptin Immunoassay (R&D Systems, Minneapolis, MN, USA), respectively. All assays were performed according to manufacturer protocols.

### Intraperitoneal glucose tolerance test and insulin tolerance test

Glucose tolerance test (GTT) and insulin tolerance test (ITT) were performed using HFD-fed *Wwp1* WT and KO

mice at 13–15 weeks old. Prior to GTT and ITT, mice were fasted for 24 h. D-glucose (1.0 g/kg body weight, Wako) or insulin (1.0 U/mL body weight, Wako) were injected intraperitoneally for GTT or ITT, respectively. Next, serial blood sampling from the tail vein was performed at 0, 30, 60, and 120 min after injection. Blood glucose levels were measured using an Accu-chek<sup>®</sup> aviva blood glucose meter (Roche).

### Measurement of glutathione concentrations

Total glutathione (tGSH [GSH + glutathione disulfide (GSSG)]) and GSSG concentrations were measured as previously reported [25]. WAT was homogenized in extraction buffer (0.1M potassium phosphate buffer containing 5 mM EDTA (pH 7.5), 0.1% Triton X-100, and 0.6% sulfosalicylic acid) and centrifuged at 4°C for 10 min. Supernatants were used for the measurement of tissue GSH content with an Infinite F200 PRO microplate reader (Tecan; Männedorf, Switzerland). The rate of 5,5-dithio-bis-(2-nitrobenzoic) acid (DTNB) formation was calculated, and the concentrations of tGSH and GSSG in each sample were determined using linear regression, with reference to a standard curve. GSH concentration was calculated by subtracting GSSG concentration from tGSH concentration.

### Measurement of citrate synthase activity

To prepare lysates for the measurement of mitochondrial activity, WAT samples were homogenized in homogenization buffer containing 50 mM Tris-HCl, pH 7.4, 150 mM NaCl, 1% phosphatase inhibitor cocktail (Thermo), 5 mM EDTA, 1% protease inhibitor cocktail (Sigma), 1% NP-40, and 0.05% sodium deoxycholate. Protein concentration in each lysate was determined using a BCA protein assay kit (Thermo Scientific; IL, USA), according to the manufacturer's protocol. Citrate synthase (CS) activity was measured by monitoring color development associated with thio-bis-(2-nitrobenzoic) acid (TNB) generation from reduction of DTNB by CoA-SH, the byproduct of citrate synthesis [24]. After addition of reaction buffer, samples were incubated at 25°C for 5 min, and the reaction was initiated by addition of 0.5 mM oxaloacetate. Changes in absorbance at 412 nm were recorded for at least 3 min using an ARVO MX/Light Wallac 1420 Multilabel/Luminescence Counter (PerkinElmer; MA, USA).

### Measurement of mitochondrial DNA content

DNA was separated and subjected to quantitative PCR using primers for *CoxII* (cytochrome c oxidase subunit II), which is encoded by mitochondrial DNA (mtDNA) (forward, 5'-CCA TCC CAG GCC GAC TAA-3'; reverse, 5'-AAT TTC AGA GCA TTG GCC ATA GA-3') or for *Hprt* (hypoxanthine guanine phosphoribosyl transferase),

which is encoded by genomic DNA (forward, 5'-ATC CAG GTT ACA AGG CAG CT-3'; reverse, 5'-GGG AAA CAT AGA CAG GGG-3'). Quantitative PCR was performed using the CFX Connect<sup>™</sup> Real Time System (Bio-Rad) and Thunderbird SYBR qPCR mix (Toyobo), according to manufacturer protocols. Relative mitochondrial copy number is represented by the amplification ratio of *CoxII* to *Hprt*.

### Measurement of oxygen consumption rate

Oxygen consumption rate (OCR) was measured as previously reported [25] in 3T3-L1/shGFP and 3T3-L1/shWwp1 cell lines after differentiation into mature adipocytes. The measurement was made using a Seahorse XF analyzer (Agilent Technologies, Santa Clara, CA, USA), according to the manufacturer's protocol.

### Statistical analysis

The Tukey–Kramer test was used to analyze data, using R software (R project for Statistical Computing). Differences with *P* values < 0.05 were considered statistically significant.

## Results

Deletion of WWP1 in WAT of *Wwp1* KO mice was confirmed at the protein level (Fig. S1A). Under ND- and HFD-fed conditions, *Wwp1* KO mice showed no differences in body mass, caloric intake, or WAT mass (Fig. S1B–D).

To evaluate the levels of oxidative stress in WAT, we measured the GSH/GSSG ratio and concentration of 4-HNE adduct, which are widely used markers of oxidative stress. HFD-fed *Wwp1* KO mice had significantly higher GSSG concentrations and lower GSH/GSSG ratio than WT mice, and these differences were not observed in ND-fed mice (Fig. 1A–C). However, WAT 4-HNE adduct concentrations were similar in all groups (Fig. 1D). These results suggest that WWP1 contributes to the antioxidative response in obese WAT.

To determine whether WWP1 affects oxidative stress by influencing mitochondrial function, we measured the enzymatic activity of CS, a rate-limiting enzyme in the TCA cycle, and the level of mtDNA, a surrogate for mitochondrial content. We found that CS activity was higher in HFD-fed mice and lower in *Wwp1* KO mice than in WT mice (Fig. 2A). In contrast, *Wwp1* KO mice showed no significant differences from WT mice in mtDNA levels under both ND- and HFD-fed conditions (Fig. 2B). These results suggest that



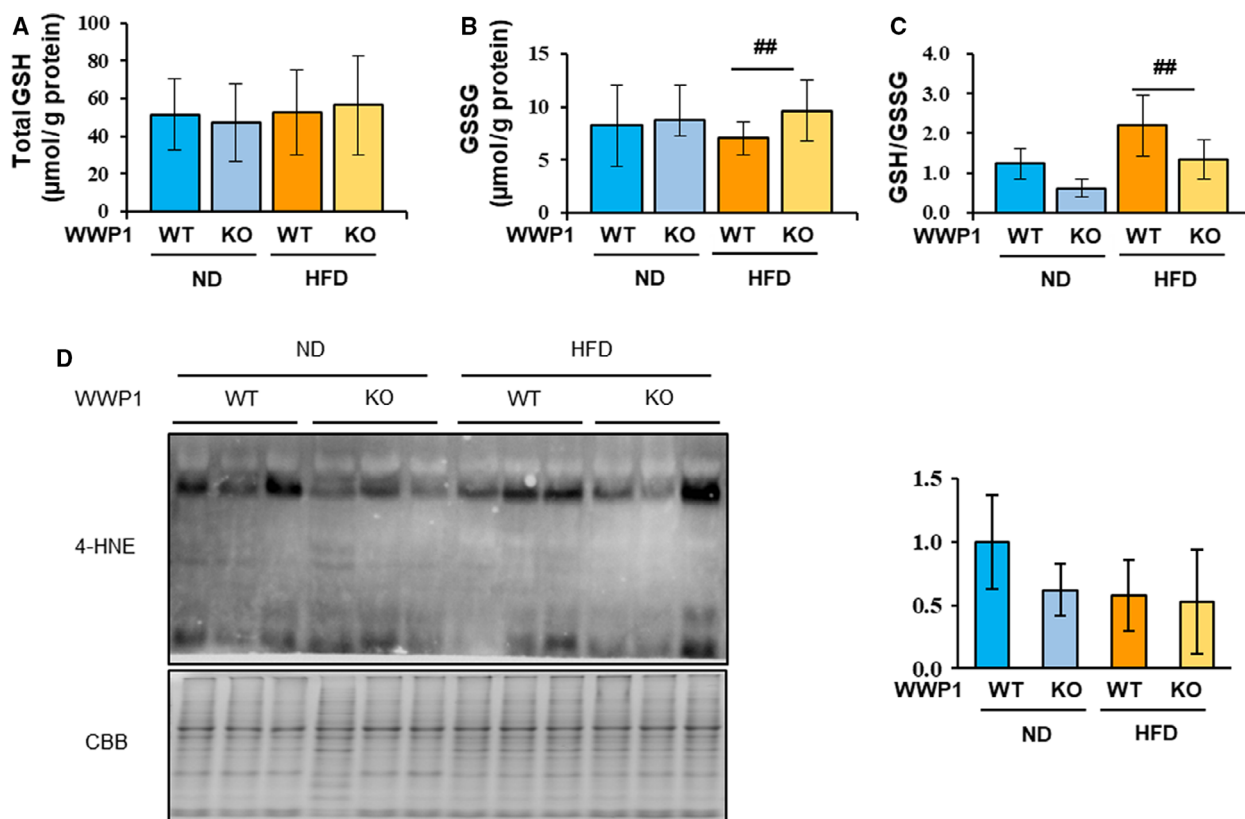


**Fig. 1.** WWP1 is involved in antioxidative reactions in obese WAT. (A–C) Glutathione concentrations in WAT from all groups of mice were measured spectrophotometrically at 412 nm. (A) total GSH, (B) GSSG, (C) GSH/GSSG ratio. (D) Immunoblotting of 4-HNE in WAT lysates from all groups of mice. CBB staining was used as the loading control. Quantitative values represent mean  $\pm$  SD ( $n = 3–5$  per group). Differences between these values were analyzed using the Tukey–Kramer test [##,  $P < 0.01$  *Wwp1* WT mice (HFD-fed) vs. *Wwp1* KO mice (HFD-fed)].

WWP1 may influence mitochondrial activity, but not mitochondrial mass, in WAT.

Obesity-induced ROS accumulation attenuates insulin signal transduction in WAT [26,27]. To assess the effects of WWP1 on insulin signaling, we measured AKT phosphorylation (pAKT), a major intermediate of insulin signaling, and plasma glucose and insulin levels in WAT from *Wwp1* WT and KO mice. The results showed that HFD-feeding induced a significant reduction in the pAKT/total AKT ratio, which was more marked in KO mice (Fig. 3A). Plasma insulin levels were decreased, but glucose levels were unchanged in KO mice (Fig. 3B,C). We performed GTT and ITT. Unexpectedly, both tests improved in KO mice, and WWP1 deficiency appeared to improve glucose metabolism (Fig. 3D–G).

Increased oxidative stress in adipose tissue is strongly associated with physiological processes and properties of adipocytes such as cell hypertrophy and adipokine imbalance. We examined mRNA levels of

adipokines (*Adipoq* (an adipocyte differentiation marker), *Leptin*), and *Ppar $\gamma$* , and plasma leptin levels. Although there were no changes in *Adipoq* levels, *Leptin* levels were increased, while *Ppar $\gamma$*  levels were decreased in the HFD groups (Fig. 4A–C). Similarly, plasma leptin levels were increased in the HFD groups (Fig. 4D). These factors were unchanged in *Wwp1* KO mice.

## Discussion

In the present study, we showed that WWP1 deficiency reduced the GSH/GSSG ratio because of increased concentration of GSSG in obese WAT. GSH is a tripeptide that contributes to reduction of concentrations of ROS, such as hydrogen peroxide and lipid peroxide [28]. An acute increase in ROS rapidly converts GSH to GSSG, resulting in a reduction of GSH/GSSG, without a change in total GSH. In contrast, chronic excess of ROS increases total GSH content,

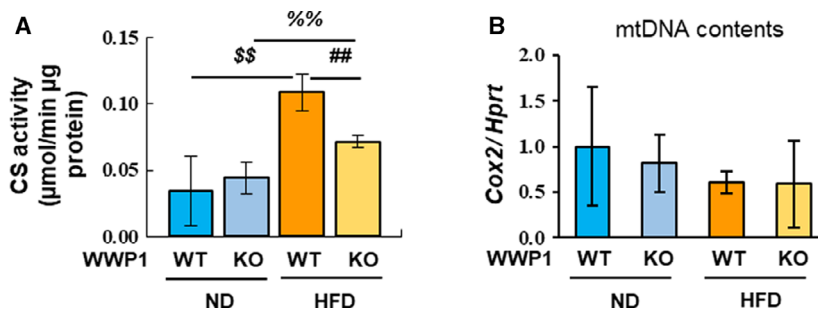


**Fig. 2.** The WWP1 is required for normal mitochondrial function in obese WAT. (A) CS activity in WAT from all groups of mice was measured spectrophotometrically at 412 nm. (B) Genomic *Cox2* levels were quantified using real-time PCR ( $n = 3-5$ ). Quantitative values represent mean  $\pm$  SD. Differences between these values were analyzed using the Tukey–Kramer test [##,  $P < 0.01$  *Wwp1* WT mice (HFD-fed) vs. *Wwp1* KO mice (HFD-fed); \$\$,  $P < 0.01$  *Wwp1* WT mice (ND-fed) vs. *Wwp1* WT mice (HFD-fed); %%,  $P < 0.01$  *Wwp1* KO mice (ND-fed) vs. *Wwp1* KO mice (HFD-fed)].

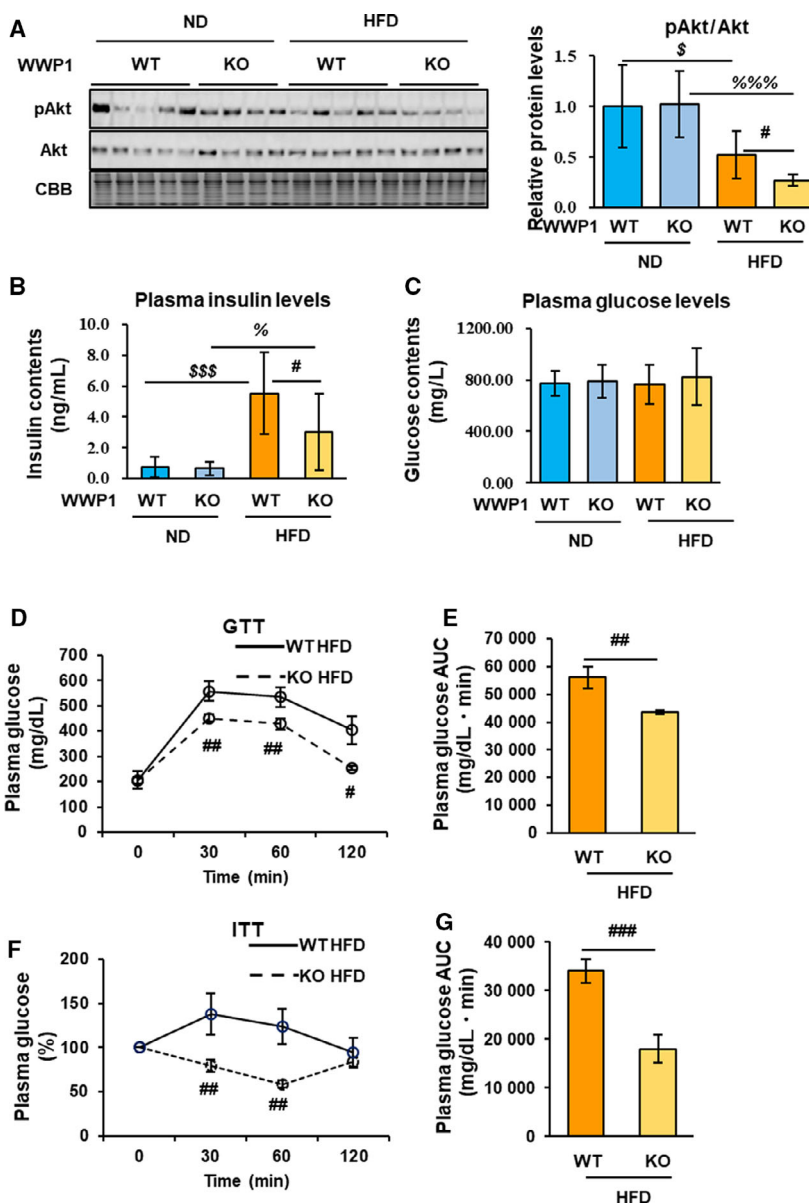


**Fig. 3.** The WWP1 contributes to the maintenance of insulin sensitivity in obese WAT. (A) Immunoblotting for phosphorylated AKT (pAKT) and total AKT in WAT from all groups of mice. (B, C) Plasma insulin (B) and glucose (C) levels from all groups of mice. (D–G) Blood glucose levels during GTT (D) or ITT (F) in HFD-fed *Wwp1* WT and KO mice. Each area under the curve (AUC) is calculated and shown as (E) or (G). Quantitative data represent mean  $\pm$  SD ( $n = 4-6$  per group). Differences between these values were analyzed using the Tukey–Kramer test [#,  $P < 0.05$ , ##,  $P < 0.01$ , ###,  $P < 0.001$ , *Wwp1* WT mice (HFD-fed) vs. *Wwp1* KO mice (HFD-fed); \$,  $P < 0.05$ , \$\$,  $P < 0.001$  *Wwp1* WT mice (ND-fed) vs. *Wwp1* WT mice (HFD-fed); %%,  $P < 0.001$  *Wwp1* KO mice (ND-fed) vs. *Wwp1* KO mice (HFD-fed)].

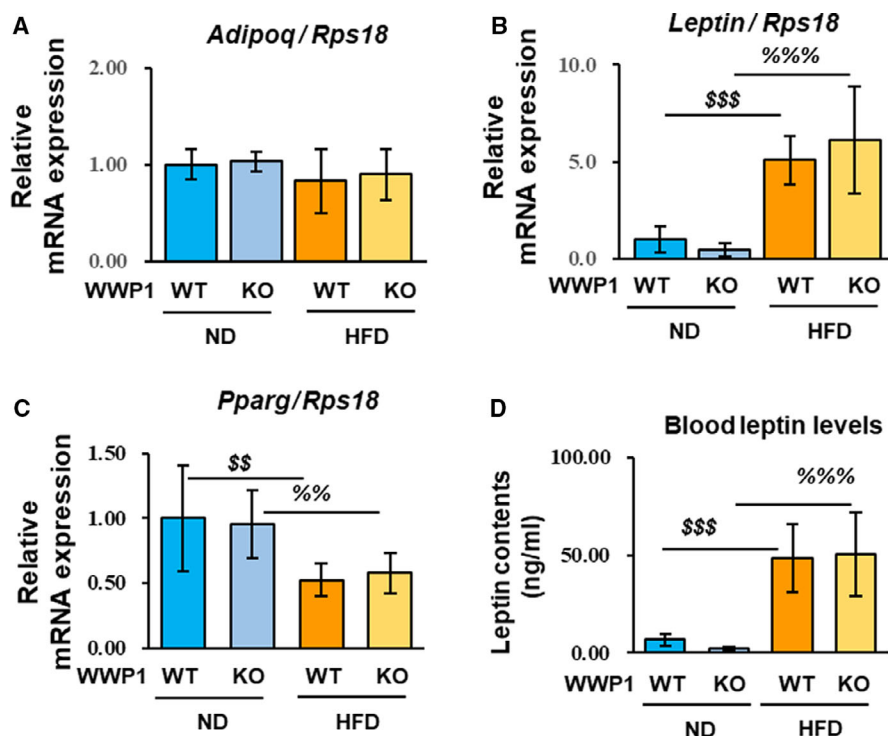


**Fig. 4.** The WWP1 contributes minimally to the regulation of adipokines and *Pparg* in obese WAT. (A–C) mRNA levels of adipokines (A) *Adipoq* and (B) *Leptin*, and (C) *Pparg* in WAT from all groups of mice were measured. (D) Plasma leptin levels from all groups of mice were measured by ELISA. Quantitative data represent mean  $\pm$  SD ( $n = 6$ –10 per group). Differences between these values were analyzed using the Tukey–Kramer test [\$\$,  $P < 0.01$ , \$\$\$,  $P < 0.001$  *Wwp1* WT mice (ND-fed) vs. *Wwp1* WT mice (HFD-fed); %,  $P < 0.01$ , %%,  $P < 0.001$  *Wwp1* KO mice (ND-fed) vs. *Wwp1* KO mice (HFD-fed)].

which increases the antioxidant capacity of tissue [29]. *Wwp1* KO mice showed normal total GSH content when fed the HFD, indicating that WWP1 may contribute to the acute antioxidative response in WAT during the early stages of obesity. This discrepancy is supported by our previously generated proteomic data, which showed that WWP1 positively regulates the expression of antioxidative proteins [23]. We also found that 4-HNE concentrations were similar in WT and KO mice and in the ND- and HFD-fed groups. As an end-product of lipid peroxidation, 4-HNE can be considered a biomarker of chronic or cumulative oxidative stress [30]. Given the above findings, it is plausible that HFD-feeding for 8 weeks induces acute oxidative stress in WAT, but does not fully induce chronic oxidative stress, while WWP1 ameliorates the acute stress. In addition, we measured the levels of antioxidative factors, such as *Txn1/2*, *Prdx1*, *Sod1/2*, and *Catalase* (Fig. S2A–F), although they were unchanged in WAT of *Wwp1* WT and KO mice. In a recent report, we showed that antioxidative factors (e.g., TRX and PRDX) correlated with WWP1 expression according to proteome analysis *in vitro*. However, we

were unable to identify any significant changes in protein expression from western blot analysis [23]. To our knowledge, the WWP1 substrates that directly contribute to the oxidative stress response have not yet been identified, although T $\beta$ R1 and Smad2, WWP1 substrates involved in TGF $\beta$  (transforming growth factor  $\beta$ ) signaling, are reported to be associated with the oxidative stress pathway [11,31]. Therefore, a comprehensive analysis of *Wwp1* WT and KO mice is required to elucidate the mechanisms involved in the WWP1-related antioxidative response.

As described above, ROS are predominantly generated in mitochondria. CS is an important enzyme in the TCA cycle, and its activity is used as a biomarker of mitochondrial function [32]. In general, both CS activity and mitochondrial mass decrease in obesity, and CS activity correlates with mitochondrial mass. However, it has been previously reported that short-term HFD-feeding increases CS activity in skeletal muscle [33]. This finding suggests that a compensatory upregulation in mitochondrial function may occur to protect against the effects of overnutrition. The findings in skeletal muscle and the present observations

regarding oxidative stress in WAT suggest that HFD increases CS activity without increasing mitochondrial mass, while WWP1 deficiency prevents full induction of CS activity in HFD-fed mice. We also found that WWP1 knockdown reduced maximal respiration in 3T3-L1 adipocytes (Fig. S3), which was consistent with the *in vivo* data.

Several previous studies have demonstrated a relationship between oxidative stress and insulin signaling. For example, it has been shown that increased mitochondrial ROS production inhibits binding of insulin receptor substrate-1 to the insulin receptor, resulting in insulin resistance [26].

This implies that lower pAKT levels in the WAT of *Wwp1* KO mice may be attributed to cumulative oxidative stress. However, while plasma insulin levels were also lower, glucose levels were not increased in KO mice. This observation suggests WWP1 deficiency can improve glucose metabolism. Consistent with these findings, GTT and ITT suggested that WWP1 deficiency can improve whole-body glucose metabolism in obesity. It is reported that WWP1 reduces the activity of phosphatase and tensin homolog (PTEN), which inhibits AKT phosphorylation [34]. Therefore, WWP1 deficiency may inhibit PTEN suppression, resulting in reduction of pAkt in *Wwp1* KO WAT. In contrast, according to GTT and ITT, whole-body glucose metabolism was improved. Because the mice analyzed in this study did not have adipose tissue-specific KO of *Wwp1*, it cannot be ruled out that WWP1 deletion affected insulin sensitivity in tissues other than WAT (e.g., liver, skeletal muscle, and brain) and secretion of insulin from pancreatic  $\beta$ -cells.

In this study, the levels of *Leptin* mRNA and plasma leptin were increased in the HFD groups, but *Adipoq* mRNA levels, which are widely known to be downregulated under conditions of obesity, were unchanged. A recent study in mice with HFD-induced obesity demonstrated that a decrease in leptin levels occurs within 8 weeks of starting the HFD, whereas the decrease of adiponectin occurs over 20 weeks [35]. This report supports the validity of our results from mice fed with a HFD for 8 weeks. Increased leptin levels and decreased *Ppar $\gamma$*  levels are generally observed in obesity [36,37]. However, we did not observe an effect on these factors related to *Wwp1* KO obese WAT. Therefore, we concluded that WWP1 or its related antioxidative properties exert minimal effects on adipocytes.

In our previous study, we identified WWP1 as an obesity-induced factor that positively regulates antioxidative reactions in adipocytes [23]. Consistent with these findings, in the present study, we showed that

*Wwp1* KO mice exhibit lower obesity-responsive antioxidant capacity. We also showed that *Wwp1* KO mice have poorer mitochondrial function and insulin signaling capacity. Therefore, we conclude that WWP1 may be involved in maintaining WAT function, including the response to oxidative stress, mitochondrial function, and insulin signaling in obesity. Further investigation of the role of WWP1 in WAT should provide insight into obesity-related pathology in WAT. In particular, identification of the WWP1 substrates should be prioritized.

## Acknowledgements

We thank all members of the laboratory of Molecular Pathology and Metabolic Disease for their cooperation. This work was supported by a Grant-in-Aid for Scientific Research (B) to Y.H. (grant number 17H02179) and by a Grant-in-Aid for Young Scientists (B) to M.K. (grant number 17K13231) from the Japan Society for the Promotion of Science; and by the MEXT Program for Strategic Research at Private Universities, 2014–2018. We also thank Mark Cleasby, PhD, and Richard Robins, PhD, from Edanz Group ([www.edanzediting.com/ac](http://www.edanzediting.com/ac)) for editing a draft of this manuscript.

## Author contributions

MK and YH conceived the idea, designed experiments, and wrote the manuscript. SH predominantly performed experiments and wrote the manuscript under the leadership of MK and RT. RK, TA, KF, KM, and HW assisted with the experiments. NO and YS contributed to the discussion. YM, YN, TN, and HK supported the experiments.

## Conflict of interest

The authors declare no conflict of interest.

## References

- 1 Furukawa S, Fujita T, Shimabukuro M, Iwaki M, Yamada Y, Nakajima Y, Nakayama O, Makishima M, Matsuda M and Shimomura I (2003) Increased oxidative stress in obesity and its impact on metabolic syndrome. *J Clin Invest* **114**, 1752–1761.
- 2 Pagliarunga S, Ludzki A, Root-McCaig J and Holloway GP (2015) In adipose tissue, increased mitochondrial emission of reactive oxygen species is important for short-term high-fat diet-induced insulin resistance in mice. *Diabetologia* **58**, 1071–1080.



- 3 Stadman ER and Levine RL (2003) Free radical-mediated oxidation of free amino acids and amino acid residues in proteins. *Amino Acids* **25**, 207–218.
- 4 Richter C, Park JW and Ames BN (1988) Normal oxidative damage to mitochondrial and nuclear DNA is extensive. *Proc Natl Acad Sci USA* **85**, 6465–6467.
- 5 Rubbo H, Denicola A and Radi R (1994) Peroxynitrite inactivates thiol-containing enzymes of *Trypanosoma cruzi* energetic metabolism and inhibits cell respiration. *Arch Biochem Biophys* **308**, 96–102.
- 6 Sakuraba H, Mizukami H, Yagihashi N, Wada R, Hanyu C and Yagihashi S (2002) Reduced beta-cell mass and expression of oxidative stress-related DNA damage in the islet of Japanese Type II diabetic patients. *Diabetologia* **45**, 85–96.
- 7 Fernández-Sánchez A, Madrigal-Santillán E, Bautista M, Esquivel-Soto J, Morales-González A, Esquivel-Chirino C, Durante-Montiel I, Sánchez-Rivera G, Valadez-Vega C and Morales-González JA (2011) Inflammation, oxidative stress, and obesity. *Int J Mol Sci* **12**, 3117–3132.
- 8 Kostapanos MS, Spyrou AT, Tellis CC, Gazi IF, Tselepis AD, Elisaf M and Liberopoulos EN (2011) Ezetimibe treatment lowers indicators of oxidative stress in hypercholesterolemic subjects with high oxidative stress. *Lipids* **46**, 341–348.
- 9 Manna P and Jain SK (2015) Obesity, oxidative stress, adipose tissue dysfunction, and the associated health risks: causes and therapeutic strategies. *Metab Syndr Relat Disord* **13**, 423–444.
- 10 Chattopadhyay M, Khemka VK, Chatterjee G, Ganguly A, Mukhopadhyay S and Chakrabarti S (2015) Enhanced ROS production and oxidative damage in subcutaneous white adipose tissue mitochondria in obese and type 2 diabetes subjects. *Mol Cell Biochem* **399**, 95–103.
- 11 Seo SR, Lallemand F, Ferrand N, Pessah M, L'Hoste S, Camonis J and Atfi A (2004) The novel E3 ubiquitin ligase Tiull1 associates with TGIF to target Smad2 for degradation. *EMBO J* **23**, 3780–3792.
- 12 Zhi X and Chen C (2012) WWP1: a versatile ubiquitin E3 ligase in signaling and diseases. *Cell Mol Life Sci* **69**, 1425–1434.
- 13 Chen C, Zhou Z, Ross JS, Zhou W and Dong JT (2007) The amplified WWP1 gene is a potential molecular target in breast cancer. *Int J Cancer* **121**, 80–87.
- 14 Imamura M, Nakamura A, Mannen H and Takeda S (2016) Characterization of WWP1 protein expression in skeletal muscle of muscular dystrophy chickens. *J Biochem* **159**, 171–179.
- 15 Hirata Y, Nomura K, Senga Y, Okada Y, Kobayashi K, Okamoto S, Minokoshi Y, Imamura M, Takeda S, Hosooka T *et al.* (2019) Hyperglycemia induces skeletal muscle atrophy via a WWP1/KLF15 axis. *J.C.I. Insight* **4**, e124952.
- 16 Ambrozkiwicz MC, Schwark M, Kishimoto-Suga M, Borisova E, Hori K, Salazar-Lázaro A, Rusanova A, Altas B, Piepkorn L, Bessa P *et al.* (2018) Polarity acquisition in cortical neurons is driven by synergistic action of Sox9-regulated Wwp1 and Wwp2 E3 ubiquitin ligases and intronic miR-140. *Neuron* **100**, 1097–1115.
- 17 Conkright MD, Wani MA and Lingrel JB (2001) Lung Krüppel-like factor contains an autoinhibitory domain that regulates its transcriptional activation by binding WWP1, an E3 ubiquitin ligase. *J Biol Chem* **276**, 29299–29306.
- 18 Zhang X, Srinivasan SV and Lingrel JB (2004) WWP1-dependent ubiquitination and degradation of the lung Krüppel-like factor KLF2. *Biochem Biophys Res Commun* **316**, 139–148.
- 19 Chen C, Sun X, Guo P, Dong XY, Sethi P, Cheng X, Zhou J, Ling J, Simons JW, Lingrel JB *et al.* (2005) Human Krüppel-like factor 5 is a target of the E3 ubiquitin ligase WWP1 for proteolysis in epithelial cells. *J Biol Chem* **280**, 41553–41561.
- 20 Eastman SW, Yassaee M and Bieniasz PD (2009) A role for ubiquitin ligases and Spartin/SPG20 in lipid droplet turnover. *J Cell Biol* **184**, 881–894.
- 21 Edwards TL, Clowes VE, Tsang HT, Connell JW, Sanderson CM, Luzio JP and Reid E (2009) Endogenous spartin (SPG20) is recruited to endosomes and lipid droplets and interacts with the ubiquitin E3 ligases AIP4 and AIP5. *Biochem J* **423**, 31–39.
- 22 Oishi Y, Manabe I, Tobe K, Ohsugi M, Kubota T, Fujii K, Maemura K, Kubota N, Kadowaki T and Nagai R (2008) SUMOylation of Krüppel-like transcription factor 5 acts as a molecular switch in transcriptional programs of lipid metabolism involving PPAR- $\delta$ . *Nat Med* **14**, 656–666.
- 23 Kobayashi M, Hoshino S, Abe T, Okita N, Tagawa R, Nagai W, Konno R, Suzuki Y, Furuya K, Ishikawa N *et al.* (2019) Identification of WWP1 as an obesity-associated E3 ubiquitin ligase with a protective role against oxidative stress in adipocytes. *Biochem Biophys Res Commun* **508**, 117–122.
- 24 Okita N, Hayashida Y, Kojima Y, Fukushima M, Yuguchi K, Mikami K, Yamauchi A, Watanabe K, Noguchi M, Nakamura M *et al.* (2012) Differential responses of white adipose tissue and brown adipose tissue to caloric restriction in rats. *Mech Ageing Dev* **133**, 255–266.
- 25 Rahman I, Kode A and Biswas SK (2006) Assay for quantitative determination of glutathione and glutathione disulfide levels using enzymatic recycling method. *Nat Protoc* **1**, 3159–3165.
- 26 Imoto K, Kukidome D, Nishikawa T, Matsuhisa T, Sonoda K, Fujisawa K, Yano M, Motoshima H, Taguchi T, Tsuruzoe K *et al.* (2006) Impact of mitochondrial reactive oxygen species and apoptosis

- signal-regulating kinase 1 on insulin signaling. *Diabetes* **55**, 1197–1204.
- 27 Mlinar B and Marc J (2011) New insights into adipose tissue dysfunction in insulin resistance. *Clin Chem Lab Med* **49**, 1925–1935.
- 28 Wu G, Fang YZ, Yang S, Lupton JR and Turner ND (2004) Glutathione metabolism and its implications for health. *J Nutr* **134**, 489–492.
- 29 Asensi M, Sastre J, Pallardo FV, Lloret A, Lehner M, Garcia-de-la Asuncion J and Viña J (1999) Ratio of reduced to oxidized glutathione as indicator of oxidative stress status and DNA damage. *Methods Enzymol* **299**, 267–276.
- 30 Kim CS, Lee SC, Kim YM, Kim BS, Choi HS, Kawada T, Kwon BS and Yu R (2008) Visceral fat accumulation induced by a high-fat diet causes the atrophy of mesenteric lymph nodes in obese mice. *Obesity* **16**, 1261–1269.
- 31 Komuro A, Imamura T, Saitoh M, Yoshida Y, Yamori T, Miyazono K and Miyazawa K (2004) Negative regulation of transforming growth factor-beta (TGF-beta) signaling by WW domain-containing protein 1 (WWP1). *Oncogene* **23**, 6914–23.
- 32 Wiegand G and Remington SJ (1986) Citrate synthase: structure, control, and mechanism. *Annu Rev Biophys Chem* **15**, 97–117.
- 33 Li X, Higashida K, Kawamura T and Higuchi M (2016) Alternate-day high-fat diet induces an increase in mitochondrial enzyme activities and protein content in rat skeletal muscle. *Nutrients* **8**, 203.
- 34 Lee YR, Chen M, Lee JD, Zhang J, Lin SY, Fu TM, Chen H, Ishikawa T, Chiang SY, Katon J *et al.* (2019) Reactivation of PTEN tumor suppressor for cancer treatment through inhibition of a MYC-WWP1 inhibitory pathway. *Science* **364**, eaau0159.
- 35 Kwon EY, Shin SK, Cho YY, Jung UJ, Kim E, Park T, Park JH, Yun JW, McGregor RA, Park YB *et al.* (2012) Time-course microarrays reveal early activation of the immune transcriptome and adipokine dysregulation leads to fibrosis in visceral adipose depots during diet-induced obesity. *BMC Genom* **13**, 450.
- 36 Lodhi IJ, Yin L, Jensen-Urstad AP, Funai K, Coleman T, Baird JH, El Ramahi MK, Razani B, Song H, Fu-Hsu F *et al.* (2012) Inhibiting adipose tissue lipogenesis reprograms thermogenesis and PPAR $\gamma$  activation to decrease diet-induced obesity. *Cell Metab* **16**, 189–201.
- 37 Step SE, Lim HW, Marinis JM, Prokesch A, Steger DJ, You SH, Won KJ and Lazar MA (2014) Anti-diabetic rosiglitazone remodels the adipocyte transcriptome by

redistributing transcription to PPAR $\gamma$ -driven enhancers. *Genes Dev* **28**, 1018–1028.

## Supporting information

Additional supporting information may be found online in the Supporting Information section at the end of the article.

**Fig. S1.** Body mass, tissue masses, and caloric intake of *Wwp1* WT and KO mice. (A) Protein expression of WWP1. The protein levels of the indicated proteins were determined by immunoblot analysis. The data were normalized to the total protein levels, determined following CBB staining. (B) Body mass and (C) total calorie consumption of C57/BL6 *Wwp1* WT and KO mice fed a normal diet (ND) or a high-fat diet (HFD). (D) Mass of WAT in mice fed an ND or an HFD. The quantitative data are means  $\pm$  SD ( $n = 5-7$ ). The differences between these values were analyzed using the Tukey-Kramer test. (\$\$\$,  $p < 0.001$  *Wwp1* WT mice (ND-fed) vs. *Wwp1* WT mice (HFD-fed); %%%,  $P < 0.001$  *Wwp1* KO mice (ND-fed) vs. *Wwp1* KO mice (HFD-fed)).

**Fig. S2.** WWP1 does not affect of mRNA expression levels of antioxidant factors in WAT. (A–F) mRNA expression levels of antioxidant factors (A) Txn1, (B) Txn2, (C) Prdx1, (D) Sod1, (E) Sod2 and (F) Catalase in WAT from all the groups of mice were measured. Rps18 was used as a housekeeping gene. The quantitative values are means  $\pm$  SD ( $n = 7-10$  per group). Differences between these values were analyzed using the Tukey-Kramer test [\$\$,  $p < 0.01$ , \$\$\$,  $p < 0.001$  *Wwp1* WT mice (ND-fed) vs. *Wwp1* WT mice (HFD-fed); %,  $p < 0.01$ , %%%,  $p < 0.001$  *Wwp1* KO mice (ND-fed) vs. *Wwp1* KO mice (HFD-fed)].

**Fig. S3.** WWP1 is required for normal mitochondrial function in mature 3T3-L1 adipocytes. *In vitro* data from mature 3T3-L1/shGFP and 3T3-L1/*Wwp1* KD adipocytes are shown. The cells were analyzed using an XF24 analyzer. A time course for the measurement of oxygen consumption rate (OCR) is shown under proton leak conditions, following the addition of oligomycin (1  $\mu$ M), FCCP (1  $\mu$ M), and rotenone (1  $\mu$ M). Values are means  $\pm$  SD ( $n = 5$ ). Differences between these values were analyzed using Student's *t*-test (&,  $p < 0.05$  &&&,  $p < 0.001$ ; 3T3-L1/shGFP vs. 3T3-L1/*Wwp1* KD).